

# Synthesis and Biological Evaluation of (Hetero)Arylmethoxy- and Arylmethylamine-phenyl Derivatives as Potent P-glycoprotein Modulating Agents

Nicola Antonio Colabufo,<sup>\*,†</sup> Francesco Berardi,<sup>†</sup> Roberto Perrone,<sup>†</sup> Simona Rapposelli,<sup>\*,‡</sup> Maria Digiacomio,<sup>‡</sup> Michael Vanni,<sup>‡</sup> and Aldo Balsamo<sup>‡</sup>

Dipartimento Farmacochimico, Università degli Studi di Bari, Via Orabona, 4, 70125 Bari, Italy, and Dipartimento di Scienze Farmaceutiche, Università di Pisa, Via Bonanno, 6, 56126 Pisa, Italy

Received October 8, 2007

Starting from lead compounds **12b** and **28b**, previously characterized as P-glycoprotein (P-gp) modulating agents, two series of new compounds were investigated. Compounds **14a,b** and **15a,b** displayed high P-gp modulating activity in the submicromolar range ( $EC_{50}$  values from 0.25 to 0.80  $\mu\text{M}$ ). Moreover, amino derivatives **23–27** showed  $EC_{50}$  values ranging from 0.085 to 0.90  $\mu\text{M}$ . In the pyridyl series, the best result has been obtained for 4-pyridyl derivative **17b** ( $EC_{50}$  = 0.85  $\mu\text{M}$ ). The best P-gp modulating agents **14a,b**, **15a,b**, and **23–27** also have been studied for determining their breast cancer resistance protein (BCRP) inhibition activity. The results demonstrated that only the amino derivatives **23–27** displayed moderate BCRP inhibition activity.

## Introduction

The ATP-binding cassette (ABC) transporters are a transmembrane (TM) family of proteins<sup>1,2</sup> that extrudes various molecules across all cell membranes by using the ATP hydrolysis energy. These transporters efflux compounds from the cytoplasm to the outside of the cell or into an intracellular compartment such as the endoplasmic reticulum (ER), the mitochondria, or the peroxisome.<sup>3</sup>

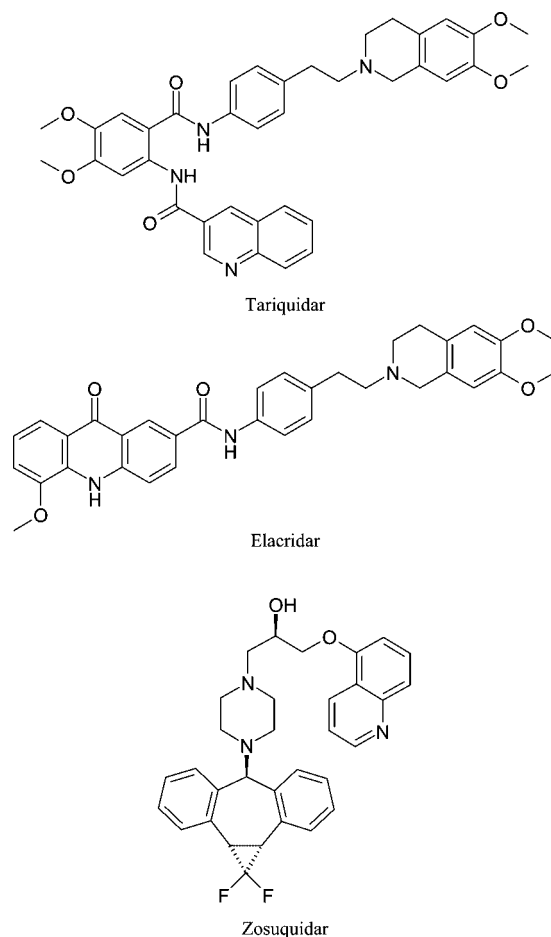
In humans, 49 ABC genes, organized into seven subfamilies (A–G), have been reported,<sup>4</sup> and many of these genes are involved in human genetic diseases<sup>5–8</sup> and in multidrug resistance (MDR).<sup>9–12</sup>

MDR is an important cause of failure of cancer treatment with chemotherapeutic agents.<sup>10,13</sup> The mechanism of MDR is mainly the cell overexpression of some ABC transporters localized in the cell membrane such as P-glycoprotein (P-gp), breast cancer resistance protein (BCRP), multidrug resistance protein 1–7 (MRP1–7), and lung resistance protein (LRP). These transporters, involved in MDR, determine this pharmacological effect by effluxing a variety of chemotherapeutic drugs from tumor cells.<sup>14</sup>

A potential strategy to reverse MDR could be the coadministration of a chemotherapeutic agent with an efflux pump inhibitor, although such reversal agents might actually increase the side effects of chemotherapy by blocking physiological anticancer drug efflux from normal cells.<sup>15–17</sup> In recent years, many drugs have been investigated for reversing MDR,<sup>18,19</sup> such as the calcium channel blocker verapamil and the antisteroids tamoxifen (first generation), biricodar (second generation), and tariquidar, elacridar, and zosuquidar (third generation), as depicted in Chart 1.

At the present, clinical trials reported elacridar<sup>20</sup> and zosuquidar<sup>21</sup> in phase I while tariquidar reached phase III, even if recently it was terminated because of an increased incidence of side effects.<sup>22</sup>

Chart 1. Third Generation P-gp Inhibitors



Recently, we developed a new class of small molecules having arylmethoxyphenyl structure that displayed moderate P-gp modulating activity.<sup>23</sup> Among these previously studied derivatives, compounds **12b** ( $EC_{50}$  = 17.2  $\mu\text{M}$ ) and **28b** ( $EC_{50}$  = 27.5  $\mu\text{M}$ ), depicted in Figure 1, have shown the best results in modulating P-gp activity. Previous studies evidenced that the P-gp inhibition activity was influenced by the presence of a

\* To whom correspondence should be addressed. (N.A.C.) Phone: +39-0805442727. Fax: +39-0805442231. E-mail: colabufo@farmchim.uniba.it. (S.R.) Phone: +39-0502219582. Fax: +39-0502219605. E-mail: rapposi@farm.unipi.it.

<sup>†</sup> Università degli Studi di Bari.

<sup>‡</sup> Università di Pisa.

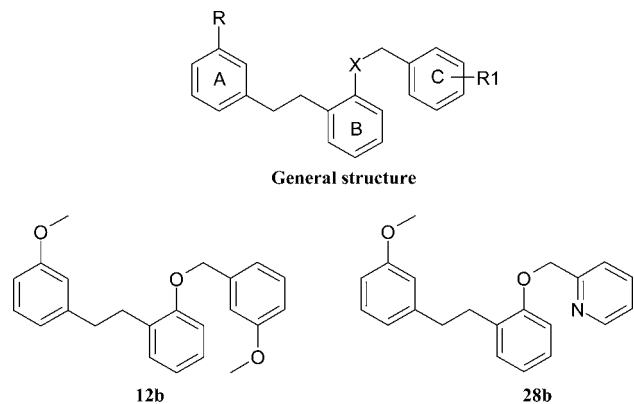
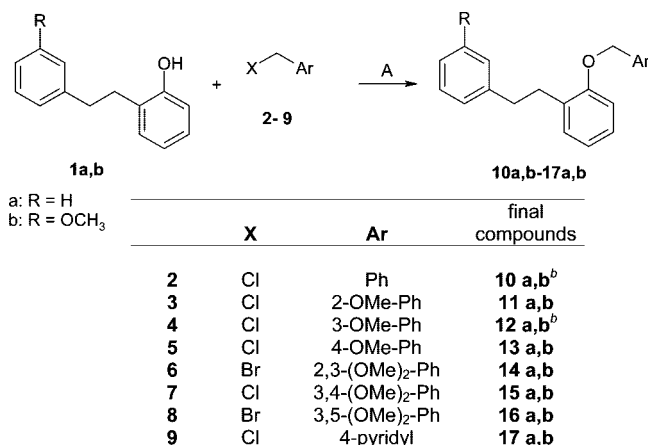


**Figure 1.** Lead compounds **12b** and **28b**.

### Scheme 1<sup>a</sup>



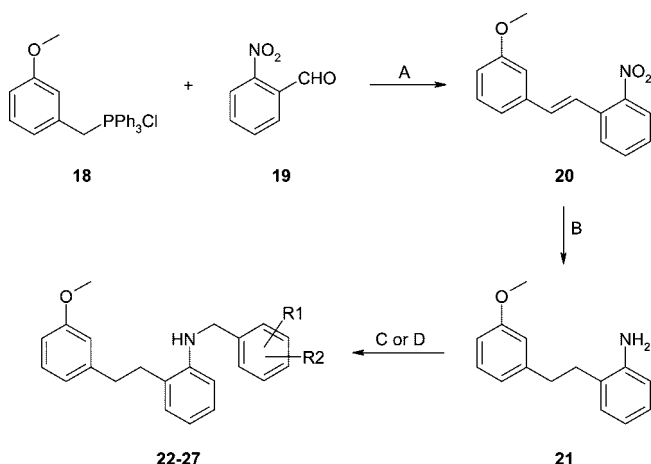
<sup>a</sup> Reagents: (A) KOH, Δ, DMSO. <sup>b</sup> Physical properties reported in ref 23.

methoxy group on the C-ring. In the present work, compounds **11a,b**, **13a,b-17a,b**, and **22-27** have been synthesized in order to investigate the following: (i) the influence of the extent of methoxylation on the C-ring for P-gp modulating activity (compounds **11a,b** and **13a,b-16a,b**), (ii) the effect of the methoxy substituent on the A-ring (**11b**, **13b-16b**, and **17b**), (iii) the effect of the position of the pyridyl nitrogen on the P-gp activity (**17a,b**), and (iv) the effect of the isosteric substitution of the oxygen in the spacer between the B-ring and C-ring with a NH group (compounds **22-27**).

The P-gp inhibition activity for each compound was studied by three combined biological assays: (i) inhibition of [<sup>3</sup>H]-vinblastine transport, (ii) ATP cell depletion, and (iii) apparent permeability (*P*<sub>app</sub>) in a Caco-2 cells monolayer. By these assays, it was possible to determine the structural requirements that favor P-gp inhibition and the mechanism involved in P-gp modulation.<sup>24</sup> Moreover, the best P-gp modulators have been tested for both their BCRP activity and cytotoxicity.

**Chemistry.** Compounds **10a,b-17a,b** were prepared by alkylation of phenols **1a,b**<sup>23</sup> with the appropriate substituted benzyl halide (**2-8**) or with 4-chloromethylpyridine (**9**) in the presence of KOH, as reported in Scheme 1. The aniline derivatives **22-27** were synthesized starting from the phosphonium salt **18**, which was submitted to Wittig's reaction with 2-nitrobenzaldehyde (**19**) to give 1-[2-(3-methoxyphenyl)vinyl]-2-nitrobenzene (**20**) as a mixture of *cis* and *trans* isomers (Scheme 2). The subsequent catalytic hydrogenation of **20** afforded the aniline derivative **21**. The final compounds **22-24** were obtained by a microwave reaction with the appropriate

### Scheme 2<sup>a</sup>



	<b>22-27</b>	
	<b>R1</b>	<b>R2</b>
<b>22</b>	2-Ome	H
<b>23</b>	3-Ome	H
<b>24</b>	4-Ome	H
<b>25</b>	2-Ome	3-Ome
<b>26</b>	3-Ome	4-Ome
<b>27</b>	3-Ome	5-Ome

<sup>a</sup> Reagents: (A) DBU (1,8-diazabicyclo[5.4.0]undec-7-ene), CH<sub>3</sub>CN; (B) H<sub>2</sub>, Pd/C 10%, EtOH; (C) appropriate methoxybenzylchloride, KI, CH<sub>3</sub>CN, microwave; (D) (i) appropriate dimethoxybenzaldehyde, EtOH, reflux, (ii) NaBH<sub>4</sub>, EtOH/H<sub>2</sub>O.

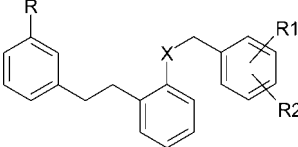
methoxybenzylchloride in the presence of a catalytic amount of KI,<sup>25</sup> while compounds **25-27** were obtained by reaction of **21** with the corresponding dimethoxy-benzaldehydes and subsequent reduction with NaBH<sub>4</sub>. The synthesis of compounds **10a,b**, **12a,b**, **28a,b**, and **29a,b** was reported in our previous work.<sup>23</sup>

## Results and Discussion

**SAR Studies.** The new compounds synthesized (**11a,b**, **13a,b-17a,b**, and **22-27**) were evaluated for their ability to inhibit the P-gp protein. Results are reported in Tables 1 and 2, together with those already obtained for the previously described analogues (**10a,b**, **12a,b**, **28a,b**, and **29a,b**) and the reference drugs (elacridar, verapamil, and cyclosporin A).

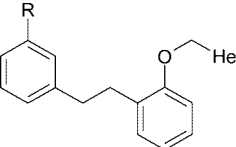
The results of the **12b** analogues (Table 1) studied for determining the importance of the presence, the position, and the extent of methoxylation of the C-ring displayed that the unsubstituted derivative **10b**<sup>23</sup> is a weak P-gp modulating agent (EC<sub>50</sub> = 92.8 μM) with respect to monosubstituted derivatives **11b-13b** (EC<sub>50</sub> = 12, 17.2, and 5.2 μM, respectively). Compound **13b**, which had the best activity, had a 4-OCH<sub>3</sub> substituent on the C-ring.

In regards to the C-ring dimethoxy-substituted derivatives (**14b-16b**), all isomers were found to be more active than the monosubstituted ones, in accord with the hypothesis that substituents able to increase the hydrogen bond formation with the P-gp active site might constitute an important structural requirement for improving the P-gp inhibition activity.<sup>26-28</sup> The best results were observed for 2,3- and 3,4-dimethoxy derivatives **14b** (EC<sub>50</sub> = 0.25 μM) and **15b** (EC<sub>50</sub> = 0.65 μM), while the 3,5-dimethoxy derivative **16b** displayed a slightly lower P-gp inhibition activity (EC<sub>50</sub> = 2.5 μM) than those of the corresponding isomers **14b** and **15b**. This trend was also confirmed by the data concerning their inferior homologues, lacking the methoxy substituent on the A-ring (**10a-16a**). In fact, also in this series, the best results were observed for 2,3- and 3,4-dimethoxy derivatives **14a** and **15a** (EC<sub>50</sub> = 0.80 and 0.75 μM,

**Table 1.** Biological Results of Derivatives **10a,b–16a,b** and **22–27**


compd	R	X	R1	R2	[ <sup>3</sup> H]-vinblastine transport inhibition, EC <sub>50</sub> ± S.E.M. (μM) <sup>a</sup>	ATP-ase activation <sup>b</sup>	[P <sub>app</sub> (B-A)]/[P <sub>app</sub> (A-B)] <sup>c</sup>
<b>10a<sup>c</sup></b>	H	O	H	H	> 1000 <sup>c</sup>	Y <sup>c</sup>	
<b>10b<sup>c</sup></b>	OCH <sub>3</sub>	O	H	H	92.8 ± 5.5 <sup>c</sup>	N <sup>c</sup>	
<b>11a</b>	H	O	2-OCH <sub>3</sub>	H	20 ± 2.5	N	1.4
<b>11b</b>	OCH <sub>3</sub>	O	2-OCH <sub>3</sub>	H	12 ± 1.5	N	8.7
<b>12a<sup>c</sup></b>	H	O	3-OCH <sub>3</sub>	H	95.6 ± 10.0 <sup>c</sup>	Y <sup>c</sup>	
<b>12b<sup>c</sup></b>	OCH <sub>3</sub>	O	3-OCH <sub>3</sub>	H	17.2 ± 0.5 <sup>c</sup>	N <sup>c</sup>	13
<b>13a</b>	H	O	4-OCH <sub>3</sub>	H	3.1 ± 0.5	N	5.1
<b>13b</b>	OCH <sub>3</sub>	O	4-OCH <sub>3</sub>	H	5.2 ± 0.50	N	7.6
<b>14a</b>	H	O	2-OCH <sub>3</sub>	3-OCH <sub>3</sub>	0.80 ± 0.05	N	0.95
<b>14b</b>	OCH <sub>3</sub>	O	2-OCH <sub>3</sub>	3-OCH <sub>3</sub>	0.25 ± 0.05	Y	7.8
<b>15a</b>	H	O	3-OCH <sub>3</sub>	4-OCH <sub>3</sub>	0.75 ± 0.07	N	2.1
<b>15b</b>	OCH <sub>3</sub>	O	3-OCH <sub>3</sub>	4-OCH <sub>3</sub>	0.65 ± 0.08	N	5.1
<b>16a</b>	H	O	3-OCH <sub>3</sub>	5-OCH <sub>3</sub>	1.60 ± 0.20	N	5.7
<b>16b</b>	OCH <sub>3</sub>	O	3-OCH <sub>3</sub>	5-OCH <sub>3</sub>	2.5 ± 0.40	N	6.7
<b>22</b>	OCH <sub>3</sub>	NH	2-OCH <sub>3</sub>	H	N.D. <sup>e</sup>	N.D. <sup>e</sup>	N.D. <sup>e</sup>
<b>23</b>	OCH <sub>3</sub>	NH	3-OCH <sub>3</sub>	H	0.48 ± 0.002	N	2.9
<b>24</b>	OCH <sub>3</sub>	NH	4-OCH <sub>3</sub>	H	N.D. <sup>e</sup>	N.D. <sup>e</sup>	N.D. <sup>e</sup>
<b>25</b>	OCH <sub>3</sub>	NH	2-OCH <sub>3</sub>	3-OCH <sub>3</sub>	0.085 ± 0.02	N	5.5
<b>26</b>	OCH <sub>3</sub>	NH	3-OCH <sub>3</sub>	4-OCH <sub>3</sub>	0.18 ± 0.04	N	5.6
<b>27</b>	OCH <sub>3</sub>	NH	3-OCH <sub>3</sub>	5-OCH <sub>3</sub>	0.90 ± 0.004	N	6.9
elacridar					2.0 <sup>d</sup>	N <sup>d</sup>	<2 <sup>d</sup>
cyclosporin A					80 ± 7.5	N	9.6
verapamil					20 ± 1.0	Y	1.2

<sup>a</sup> Data are the mean of three independent determinations, samples in triplicate. <sup>b</sup> Effect measured at 100 μM. Data are the mean of three independent determinations with samples in triplicate. <sup>c</sup> See ref 23. <sup>d</sup> See ref 24. <sup>e</sup> Not determined (chemically unstable).

**Table 2.** Biological Properties of Pyridyl Derivatives **28a,b**, **29a,b**, and **17a,b**


compd	R	Het	[ <sup>3</sup> H]-vinblastine transport inhibition, EC <sub>50</sub> ± SEM (μM) <sup>a</sup>	ATP-ase activation <sup>b</sup>	[P <sub>app</sub> (B-A)]/[P <sub>app</sub> (A-B)] <sup>c</sup>
<b>28a<sup>d</sup></b>	H	2-pyridyl	100 ± 25 <sup>d</sup>	N <sup>d</sup>	
<b>28b<sup>d</sup></b>	OCH <sub>3</sub>	2-pyridyl	27.6 ± 0.2 <sup>d</sup>	N <sup>d</sup>	
<b>29a<sup>d</sup></b>	H	3-pyridyl	125 ± 15 <sup>d</sup>	Y <sup>d</sup>	
<b>29b<sup>d</sup></b>	OCH <sub>3</sub>	3-pyridyl	>1000 <sup>d</sup>	Y <sup>d</sup>	
<b>17a</b>	H	4-pyridyl	18 ± 2.5	Y	1.3
<b>17b</b>	OCH <sub>3</sub>	4-pyridyl	0.85 ± 0.05	Y	2.1

<sup>a</sup> Data are the mean of three independent determinations (samples in triplicate), each with SEM < 10%. <sup>b</sup> Effect measured at 100 μM. Data are the mean of three independent determinations with samples in triplicate. <sup>c</sup> Data are the mean of three independent determinations, samples in triplicate. <sup>d</sup> See ref 23.

respectively), while 3,5-dimethoxy compound **16a** displayed only moderate P-gp inhibition activity (EC<sub>50</sub> = 1.60 μM).

Moreover, with respect to the dimethoxy compounds **14a–16a**, the monosubstituted derivatives **11a–13a** displayed lower activity (EC<sub>50</sub> = 20.0, 95.6, and 3.1 μM, respectively), but the latter was more potent than the unsubstituted **10a** (EC<sub>50</sub> > 1000 μM). Among monomethoxy derivatives, also in this series, the compound bearing 4-OCH<sub>3</sub> on the C-ring, **13a**, displayed the best activity.

Furthermore, comparing the biological results of compounds differing by the presence (**10b–16b**) or the absence (**10a–16a**) of the methoxy group on the A-ring, it was evident that this substituent played a modest role on the P-gp inhibition activity, with the exception of compounds **10a,b** and **12a,b**. In fact,

compound **10b** is some 10 times more potent than **10a**, and **12b** is 5.5 times more potent than **12a**.

The isosteric substitution of oxygen present on the spacer linking the B-ring to the C-ring of the lead compound **12b** with NH, as in compound **23**, determined an increase in the P-gp inhibition activity (EC<sub>50</sub> = 17.2 vs 0.48 μM, respectively). The position of the methoxy on the C-ring in this series has been evaluated. Derivatives **22** and **24** bearing 2-OCH<sub>3</sub> and 4-OCH<sub>3</sub> on the C-ring, respectively, were chemically unstable when dissolved in EtOH, DMSO, and phosphate buffered saline (PBS), which are the solvents employed in the biological assays. Among the dimethoxy-substituted derivatives **25–27**, the best P-gp inhibition activity was observed for the 2,3-dimethoxy-substituted compound **25** (EC<sub>50</sub> = 0.085 μM), while the 3,5-

dimethoxy-substituted derivative **27** displayed a slightly lower P-gp inhibition activity ( $EC_{50} = 0.90 \mu\text{M}$ ). Compound **26**, bearing a 3,4-dimethoxy substitution on the C-ring, displayed good P-gp inhibition activity ( $EC_{50} = 0.18 \mu\text{M}$ ). These results demonstrated the same trend observed for the corresponding isomers **14b–16b**, having an oxygen atom in the spacer between the B-ring and the C-ring.

Moreover, starting from the lead heteroaromatic compound **28b**, having a 2-pyridyl moiety, instead of the C-ring, the shifting of the pyridyl linkage from the 2 to the 3 and 4 positions (**29b** and **17b**, respectively) has been investigated. The results listed in Table 2 displayed that the best P-gp inhibition activity was obtained for compound **17b**, having a 4-pyridyl nucleus ( $EC_{50} = 0.85 \mu\text{M}$ ).

Moreover, the P-gp modulating activity dramatically decreased in compound **29b** where the heteroaromatic was a 3-pyridyl ( $EC_{50} > 1000 \mu\text{M}$ ). The same trend was observed also in the corresponding derivatives lacking a methoxy substituent on the A-ring (**28a**, **29a**, and **17a**). In fact, the 4-pyridyl derivative **17a** is the best of the series ( $EC_{50} = 18.0 \mu\text{M}$ ), while the 2- and 3-pyridyl derivatives **28a** and **29a** displayed weak inhibition activity ( $EC_{50} = 100$  and  $125 \mu\text{M}$ , respectively). This finding indicates a marked influence on the P-gp inhibitory activity of the position of the nitrogen atom on the pyridine nucleus.

Comparing **17a** with **17b** ( $EC_{50} = 18$  vs  $0.85 \mu\text{M}$ , respectively) and **28a** with **28b** ( $EC_{50} = 100$  vs  $27.6 \mu\text{M}$ , respectively), it was evident that the presence of a methoxy substituent on the A-ring in this series seems to be significantly involved in the P-gp modulation activity. On the other hand, compounds **29a** and **29b** were both weakly active.

**P-gp Inhibition Mechanism Investigation.** In a monolayer efflux assay, the apparent permeability ( $P_{app}$ ) in both basolateral to apical [ $P_{app}(B-A)$ ] and apical to basolateral [ $P_{app}(A-B)$ ] directions was determined for each compound. The BA/AB ratio is ranging from 0.95 to 2.1 for compounds **11a**, **14a**, **15a**, **17a,b**, and the reference compounds verapamil and elacridar (BA/AB = 1.2 and 2, respectively), while the other compounds and cyclosporin A displayed BA/AB  $> 2.9$ .

The compounds having BA/AB ratio up to 2.1 were not effluxed by P-gp, while compounds with BA/AB ratio  $> 2.9$  were P-gp transported and consequently considered substrates of this pump.<sup>24</sup>

As regards ATP-ase activation, all compounds were unable to deplete ATP from cells with the exception of **10a**, **12a**, **14b**, **17a,b**, and **29a,b**. The compounds that reduced the cell ATP level were considered P-gp substrates, while the compounds with unmodified ATP cell content were not effluxed by P-gp.

Combining the results of the biological assays, compounds **11a**, **14a**, **15a**, and the reference compound elacridar were claimed "P-gp inhibitors" because they were not transported by P-gp, they inhibited [ $^3\text{H}$ ]-vinblastine transport, and they were unable to deplete ATP.

Compounds **17a,b** as well as verapamil were not transported by P-gp; they inhibited [ $^3\text{H}$ ]-vinblastine transport, but they were able to promote the depletion of ATP so that they were claimed "not transported" P-gp substrates.

Compounds **11b**, **13a,b**, **15b**, **16a,b**, **23**, and **25–27** as well as cyclosporin A were effluxed by P-gp; they inhibited [ $^3\text{H}$ ]-vinblastine transport, and they were unable to deplete ATP so that they were considered "saturating transported" P-gp substrates.

Only compound **14b** was a P-gp substrate because it was effluxed by P-gp, it inhibited [ $^3\text{H}$ ]-vinblastine transport, and it depleted ATP.

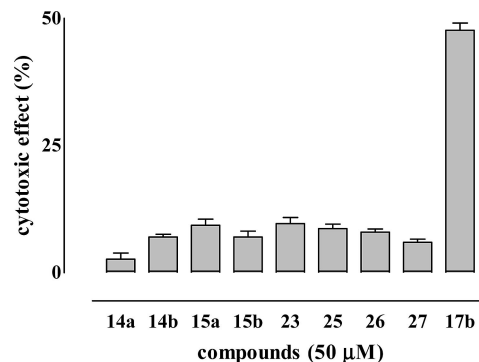


**Figure 2.** Cytotoxic effect of P-gp inhibitors on the MCF-7/Adr cell line at 48 h. The effect of compound **17b** has been determined at  $1 \mu\text{M}$ .

**Table 3.** BCRP Inhibition Evaluation of Derivatives **14a,b**, **15a**, **23**, **25**, and **26**

compd	[ $^3\text{H}$ ]-mitoxantrone transport inhibition, $EC_{50} \pm \text{SEM} (\mu\text{M})^a$
<b>14a</b>	$75 \pm 5$
<b>14b</b>	$120 \pm 20$
<b>15a</b>	$58 \pm 3$
<b>15b</b>	$150 \pm 25$
<b>23</b>	$7.0 \pm 0.5$
<b>25</b>	$1.5 \pm 0.20$
<b>26</b>	$0.50 \pm 0.02$

<sup>a</sup> Data are the mean of three independent determinations, samples in triplicate.

**Biological Cell Activity.** Since the P-gp modulators should be devoid of cytotoxic activity, we tested compounds **14a,b**, **15a,b**, **17b**, **23**, and **25–27**, displaying submicromolar activity values, to establish their intrinsic cytotoxicity in the MCF-7/Adr cell line overexpressing P-gp. As depicted in Figure 2, all tested compounds until  $50 \mu\text{M}$  were devoid of cytotoxicity at 48 h, except compounds **15a** and **23**, which displayed only moderate cytotoxicity (10%). In contrast, compound **17b** displayed high cytotoxicity (50%) at  $1 \mu\text{M}$  (Figure 2, last bar to the right), so that this result discouraged the development of the pyridyl series as potential MDR reverting agents.

**BCRP Activity.** Since the limit of P-gp inhibitors such as elacridar is the poor selectivity toward other ABC transporters, in particular the BCRP pump, the best P-gp modulators, **14a,b**, **15a,b**, **23**, **25**, and **26**, were tested for their ability to inhibit [ $^3\text{H}$ ]-mitoxantrone, a specific BCRP substrate. In Table 3 are reported the  $EC_{50}$  values of these compounds. The results showed that oxygen derivatives **14a,b** and **15a,b** were weakly active to inhibit the BCRP pump ( $EC_{50}$  from 58 to  $150 \mu\text{M}$ ). In contrast, the amino derivatives **23**, **25**, and **26** showed a good BCRP inhibition activity. In particular, compounds **25** and **26** showed micromolar BCRP inhibition activity ( $EC_{50} = 1.5$  and  $0.5 \mu\text{M}$ , respectively).

## Conclusions

In our previous work, we studied arylmethoxyphenyl derivatives displaying P-gp modulating activity, and among them **12b** and **28b** were suggested as lead compounds of this new class of small P-gp modulators. Starting from **12b**, the extent of methoxylation on the C-ring, the effect of a methoxy substituent on the A-ring, and the influence of isosteric substitution have been investigated.

Starting from **28b**, the effect of 3- and 4-pyridyl isomers and the influence of a methoxy substituent on the A-ring have

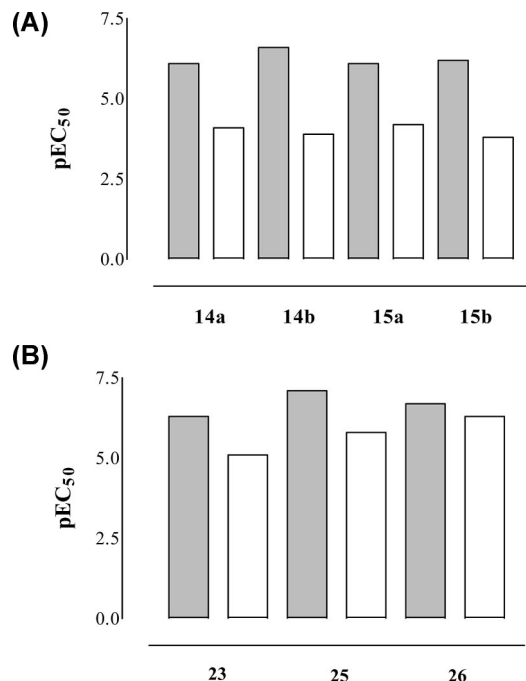


**Figure 3.** Comparison between P-gp (gray bars) and BCRP (white bars) inhibition activity of oxygen derivatives (A) and amino derivatives (B).

been studied. As expected, the extent of methoxylation on the C-ring improved the P-gp inhibition activity both in the series lacking a methoxy group (**14a–16a**) and in the corresponding series bearing a methoxy group (**14b–16b**) on the A-ring. However, the presence of a methoxy on the A-ring slightly potentiated P-gp inhibition activity. Among dimethoxy substitutions on the C-ring, the best results have been obtained for the 2,3- and 3,4-*ortho*-disubstituted derivatives, while 3,5-disubstituted derivatives were less active in all of the series. The effect of the methoxy position on the C-ring in monosubstituted derivatives has been investigated, demonstrating that the *para*-substitution determined the best activity toward P-gp in all series, although these compounds were less active than the corresponding disubstituted derivatives. The best results in inhibiting P-gp were obtained for the amino derivatives bearing a methoxy substituent on the A-ring, which are always more potent than the corresponding oxygen derivatives. Also in this series, 2,3- and 3,4-*ortho*-disubstituted derivatives on the C-ring showed the highest P-gp inhibition values in the nanomolar range ( $EC_{50} = 0.085 \mu\text{M}$  for compound **25**). Considering the inhibition activity profile of some reference compounds, elacridar in particular, displaying dual inhibition activity toward P-gp and BCRP pumps, the selectivity of the best P-gp modulators has been investigated. The results displayed that both the oxygen and the amino derivatives had similar potency in inhibiting P-gp, but the oxygen derivatives were more selective toward P-gp with respect to BCRP.

In Figure 3A, for the best oxygen derivatives, the activity values (pEC<sub>50</sub>) toward P-gp and BCRP have been compared. In Figure 3B, for the best amino derivatives, the same comparison has been reported.

These findings suggest that the presence of a NH group in the side chain of the arylmethylamine derivatives increases the inhibitory activity toward P-gp but in the meantime decreases the selectivity between the two types of extrusion pumps (P-gp vs BCRP). In conclusion, the present paper suggests that suitable

chemical manipulations of this new class of P-gp inhibitors may lead to the synthesis of new derivatives endowed of improved inhibitory activity and selectivity.

## Experimental Section

**General Methods.** Melting points were determined on a Kofler hot-stage apparatus and are uncorrected. <sup>1</sup>H and <sup>13</sup>C NMR spectra were obtained with a Varian Gemini 200 MHz spectrometer. Chemical shifts ( $\delta$ ) are reported in parts per million downfield from tetramethylsilane and referenced from solvent references; coupling constants  $J$  are reported in hertz; <sup>13</sup>C NMR spectra were fully decoupled. The following abbreviations are used: singlet (s), doublet (d), triplet (t), double-doublet (dd), and multiplet (m).

Mass spectra were obtained on a Hewlett-Packard 5988 A spectrometer by using a direct injection probe and an electron beam energy of 70 eV. The elemental compositions of the compounds agreed to within  $\pm 0.4\%$  of the calculated value. Chromatographic separation was performed on silica gel columns by flash (Kieselgel 40, 0.040–0.063 mm; Merck) or gravity column (Kieselgel 60, 0.063–0.200 mm; Merck) chromatography. Reactions were followed by thin-layer chromatography (TLC) on Merck aluminum silica gel (60 F<sub>254</sub>) sheets that were visualized under a UV lamp. Evaporation was performed in vacuo (rotating evaporator). Sodium sulfate was always used as the drying agent. The microwave-assisted procedures were carried out with a CEM Discover LabMate microwave. Commercially available chemicals were purchased from Sigma-Aldrich. The UV-vis spectra of compounds **11a,b**, **13a,b–17a,b**, and **22–27**, and the corresponding calibration curves were recorded with a PerkinElmer LAMBDA BIO-20 spectrophotometer.

**General Procedure To Synthesize Final Compounds 11a,b and 13a,b–17a,b.** A solution of phenol **1a** or **1b**<sup>23</sup> (1.0 mmol) in a small amount of DMSO (2 mL) was added to a solution of KOH (174 mg, 3.11 mmol) in DMSO (2.5 mL). The mixture was stirred at room temperature for 15 min, and then a solution of the appropriate arylmethylhalide **2–9** (1.0 mmol) in DMSO (2 mL) was added dropwise to the solution of potassium 2-(2-phenylethyl)benzenolate. The suspension was stirred at room temperature for 12 h, and then it was diluted with AcOEt and washed with water and brine. The organic layer was dried and concentrated. The resulting residue was purified by chromatography on a silica gel column.

**1-[(2-Methoxybenzyl)oxy]-2-(2-phenylethyl)benzene (11a).** Purified with hexane/AcOEt (95:5) (55% yield) as a colorless oil. MS  $m/z$  318 ( $M^+$ , 85); 198 (27). <sup>1</sup>H NMR (CDCl<sub>3</sub>):  $\delta$  2.90–3.02 (m, 4H, CH<sub>2</sub>CH<sub>2</sub>), 3.90 (s, 3H, OCH<sub>3</sub>), 5.15 (s, 2H, OCH<sub>2</sub>), 6.85–7.04 (m, 4H, Ar), 7.12–7.36 (m, 8H, Ar), 7.51–7.55 (m, 1H, Ar). <sup>13</sup>C NMR (CDCl<sub>3</sub>):  $\delta$  156.99, 156.88, 142.71, 130.83, 130.08, 128.79, 128.62, 128.37, 128.31, 127.27, 126.09, 125.78, 120.70, 120.65, 112.05, 110.31, 65.55, 65.37, 36.60, 33.24. Anal. (C<sub>22</sub>H<sub>22</sub>O<sub>2</sub>) C, H. UV-vis (solvent: PBS)  $\lambda = 230 \text{ nm}$ ,  $\epsilon = 16350$ .

**1-[(2-Methoxybenzyl)oxy]-2-[2-(3-methoxyphenyl)ethyl]benzene (11b).** Purified with hexane/AcOEt (95:5) (89% yield) as a colorless oil. MS  $m/z$  348 ( $M^+$ , 62); 227 (38). <sup>1</sup>H NMR (CDCl<sub>3</sub>):  $\delta$  2.87–3.02 (m, 4H, CH<sub>2</sub>CH<sub>2</sub>), 3.75 (s, 3H, OCH<sub>3</sub>), 3.86 (s, 3H, OCH<sub>3</sub>), 5.14 (s, 2H, OCH<sub>2</sub>), 6.72–7.35 (m, 11H, Ar), 7.52 (d, 1H,  $J = 7.7 \text{ Hz}$ , Ar). <sup>13</sup>C NMR (CDCl<sub>3</sub>):  $\delta$  159.66, 156.93, 156.82, 144.31, 130.69, 130.07, 129.25, 128.78, 128.31, 127.29, 125.99, 121.04, 120.62, 114.17, 111.97, 111.43, 110.24, 65.31, 55.46, 55.24, 36.63, 33.19. Anal. (C<sub>23</sub>H<sub>24</sub>O<sub>3</sub>) C, H. UV-vis (solvent: PBS)  $\lambda = 230 \text{ nm}$ ,  $\epsilon = 16350$ .

**1-[(4-Methoxybenzyl)oxy]-2-(2-phenylethyl)benzene (13a).** Purified with hexane/Et<sub>2</sub>O (95:5) to (94% yield) as an oil. MS  $m/z$  318 ( $M^+$ , 16); 121 (100). <sup>1</sup>H NMR (CDCl<sub>3</sub>):  $\delta$  2.83–3.00 (m, 4H, CH<sub>2</sub>CH<sub>2</sub>), 3.83 (s, 3H, OCH<sub>3</sub>), 5.03 (s, 2H, OCH<sub>2</sub>), 6.85–6.95 (m, 4H, Ar), 7.11–7.40 (m, 9H, Ar). <sup>13</sup>C NMR (CDCl<sub>3</sub>):  $\delta$  159.42, 156.82, 142.58, 130.80, 130.12, 129.65, 128.94, 128.62, 128.31, 127.25, 125.79, 120.73, 114.07, 111.86, 69.91, 55.46, 36.57, 33.10. Anal. (C<sub>22</sub>H<sub>22</sub>O<sub>2</sub>) C, H. UV-vis (solvent: PBS)  $\lambda = 230 \text{ nm}$ ,  $\epsilon = 14810$ .

**1-[(4-Methoxybenzyl)oxy]-2-[2-(3-methoxyphenyl)ethyl]benzene (13b).** Purified with hexane/Et<sub>2</sub>O (4:1) (70% yield) as a semisolid. MS *m/z* 348 (M<sup>+</sup>, 55); 228 (76). <sup>1</sup>H NMR (CDCl<sub>3</sub>): δ 2.81–2.97 (m, 4H, CH<sub>2</sub>CH<sub>2</sub>), 3.74 (s, 3H, OCH<sub>3</sub>), 3.83 (s, 3H, OCH<sub>3</sub>), 5.02 (s, 2H, OCH<sub>2</sub>), 6.69–6.77 (m, 3H, Ar), 6.85–6.96 (m, 4H, Ar), 7.13–7.23 (m, 3H, Ar), 7.38 (d, 2H, *J* = 8.6 Hz, Ar). <sup>13</sup>C NMR (CDCl<sub>3</sub>): δ 159.02, 158.79, 156.18, 143.58, 130.09, 129.49, 129.0, 128.60, 128.34, 126.63, 120.40, 120.09, 113.54, 113.43, 111.21, 110.81, 69.28, 54.80, 54.58, 36.00, 32.40. Anal. (C<sub>23</sub>H<sub>24</sub>O<sub>3</sub>) C, H. UV-vis (solvent: PBS) λ = 225 nm, ε = 22560.

**1-[(2,3-Dimethoxybenzyl)oxy]-2-(2-phenylethyl)benzene (14a).** Purified with CHCl<sub>3</sub> (25% yield) as an oil. MS *m/z* 348 (M<sup>+</sup>, 65). <sup>1</sup>H NMR (CDCl<sub>3</sub>): δ 2.90–2.98 (m, 4H, CH<sub>2</sub>CH<sub>2</sub>), 3.89 (s, 3H, OCH<sub>3</sub>), 3.90 (s, 3H, OCH<sub>3</sub>), 5.16 (s, 2H, OCH<sub>2</sub>), 6.85–7.29 (m, 12H, Ar). <sup>13</sup>C NMR (CDCl<sub>3</sub>): δ 156.84, 152.63, 146.86, 142.56, 131.46, 130.67, 130.05, 128.58, 128.29, 127.29, 125.76, 124.17, 123.24, 120.71, 112.26, 111.94, 65.21, 61.10, 56.00, 36.56, 33.00. Anal. (C<sub>23</sub>H<sub>24</sub>O<sub>3</sub>) C, H. UV-vis (solvent: PBS) λ = 230 nm, ε = 22560.

**1-[(2,3-Dimethoxybenzyl)oxy]-2-[2-(3-methoxyphenyl)ethyl]benzene (14b).** Purified with CHCl<sub>3</sub> (24% yield) as an oil. MS *m/z* 378 (M<sup>+</sup>, 71). <sup>1</sup>H NMR (CDCl<sub>3</sub>): δ 2.83–3.00 (m, 4H, CH<sub>2</sub>CH<sub>2</sub>), 3.75 (s, 3H, OCH<sub>3</sub>), 3.89 (s, 3H, OCH<sub>3</sub>), 3.90 (s, 3H, OCH<sub>3</sub>), 5.17 (s, 2H, OCH<sub>2</sub>), 6.72–7.26 (m, 11H, Ar). <sup>13</sup>C NMR (CDCl<sub>3</sub>): δ 160.33, 157.49, 153.29, 147.52, 144.86, 132.11, 131.29, 130.73, 129.87, 127.96, 127.96, 124.85, 121.70, 121.41, 114.85, 112.90, 112.58, 112.10, 65.87, 61.75, 56.64, 55.88, 37.28, 33.61. Anal. (C<sub>24</sub>H<sub>26</sub>O<sub>4</sub>) C, H. UV-vis (solvent: PBS) λ = 230 nm, ε = 10420.

**1-[(3,4-Dimethoxybenzyl)oxy]-2-(2-phenylethyl)benzene (15a).** Purified with hexane/Et<sub>2</sub>O (95:5) (15% yield) as an oil. MS *m/z* 348 (M<sup>+</sup>, 25); 210 (76). <sup>1</sup>H NMR (CDCl<sub>3</sub>): δ 2.88–3.03 (m, 4H, CH<sub>2</sub>CH<sub>2</sub>), 3.84 (s, 3H, OCH<sub>3</sub>), 3.91 (s, 3H, OCH<sub>3</sub>), 5.04 (s, 2H, OCH<sub>2</sub>), 6.86–7.02 (m, 6H, Ar), 7.11–7.31 (m, 6H, Ar). <sup>13</sup>C NMR (CDCl<sub>3</sub>): δ 156.78, 149.34, 148.94, 142.49, 130.82, 130.20, 130.11, 128.51, 128.31, 127.27, 125.81, 120.84, 119.93, 111.99, 111.43, 110.99, 70.19, 56.15, 56.00, 36.54, 33.00. Anal. (C<sub>23</sub>H<sub>24</sub>O<sub>3</sub>) C, H. UV-vis (solvent: PBS) λ = 230 nm, ε = 15250.

**1-[(3,4-Dimethoxybenzyl)oxy]-2-[2-(3-methoxyphenyl)ethyl]benzene (15b).** Purified with CHCl<sub>3</sub> (16% yield) as an oil. MS *m/z* 378 (M<sup>+</sup>, 38); 227 (85). <sup>1</sup>H NMR (CDCl<sub>3</sub>): δ 2.83–3.02 (m, 4H, CH<sub>2</sub>CH<sub>2</sub>), 3.74 (s, 3H, OCH<sub>3</sub>), 3.84 (s, 3H, OCH<sub>3</sub>), 3.90 (s, 3H, OCH<sub>3</sub>), 5.03 (s, 2H, OCH<sub>2</sub>), 6.70–6.78 (m, 3H, Ar), 6.86–7.01 (m, 5H, Ar), 7.13–7.24 (m, 3H, Ar). <sup>13</sup>C NMR (CDCl<sub>3</sub>): δ 160.33, 157.42, 149.96, 149.56, 144.73, 131.37, 130.75, 129.85, 127.89, 121.57, 121.46, 120.57, 114.89, 112.61, 112.06, 111.96, 111.65, 70.81, 56.75, 56.64, 55.80, 37.21, 33.53, 31.57. Anal. (C<sub>24</sub>H<sub>26</sub>O<sub>4</sub>) C, H. UV-vis (solvent: PBS) λ = 230 nm, ε = 11350.

**1-[(3,5-Dimethoxybenzyl)oxy]-2-(2-phenylethyl)benzene (16a).** Purified with hexane/CHCl<sub>3</sub> (1:1) (26% yield) as an oil. MS *m/z* 348 (M<sup>+</sup>, 50); 198 (67). <sup>1</sup>H NMR (CDCl<sub>3</sub>): δ 2.89–3.02 (m, 4H, CH<sub>2</sub>CH<sub>2</sub>), 3.77 (s, 6H, OCH<sub>3</sub>), 5.04 (s, 2H, OCH<sub>2</sub>), 6.42 (t, 1H, *J* = 2.1 Hz, Ar), 6.62 (d, 2H, *J* = 2.1 Hz, Ar), 6.86–6.93 (m, 2H, Ar), 7.12–7.30 (m, 7H, Ar). <sup>13</sup>C NMR (CDCl<sub>3</sub>): δ 161.79, 157.35, 143.15, 140.69, 131.42, 130.82, 129.22, 128.96, 127.94, 126.47, 121.53, 112.57, 105.71, 100.61, 70.71, 56.13, 37.21, 33.68. Anal. (C<sub>23</sub>H<sub>24</sub>O<sub>3</sub>) C, H. UV-vis (solvent: PBS) λ = 230 nm, ε = 15377.

**1-[(3,5-Dimethoxybenzyl)oxy]-2-[2-(3-methoxyphenyl)ethyl]benzene (16b).** Purified with hexane/CHCl<sub>3</sub> (3:7) (43% yield) as an oil. MS *m/z* 378 (M<sup>+</sup>, 22); 227 (93). <sup>1</sup>H NMR (CDCl<sub>3</sub>): δ 2.86–3.05 (m, 4H, CH<sub>2</sub>CH<sub>2</sub>), 3.75 (s, 3H, OCH<sub>3</sub>), 3.77 (s, 6H, OCH<sub>3</sub>), 5.04 (s, 2H, OCH<sub>2</sub>), 6.42 (t, 1H, *J* = 2.3 Hz, Ar), 6.62 (d, 2H, *J* = 2.3 Hz, Ar), 6.71–6.93 (m, 4H, Ar), 7.12–7.21 (m, 4H, Ar). <sup>13</sup>C NMR (CDCl<sub>3</sub>): δ 161.79, 160.39, 157.35, 144.77, 140.67, 131.40, 130.84, 129.89, 127.96, 121.66, 121.57, 114.87, 112.59, 112.14, 105.73, 100.59, 70.75, 56.11, 55.87, 37.28, 33.60. Anal. (C<sub>24</sub>H<sub>26</sub>O<sub>4</sub>) C, H. UV-vis (solvent: PBS) λ = 230 nm, ε = 16350.

**4-[[2-(2-Phenylethyl)phenoxy]methyl]pyridine (17a).** The oil **17a** was transformed to the hydrochloride salt, a white solid (343 mg, 1.1 mmol, 56% yield). Mp: 120–122 °C. MS *m/z* 289 (M<sup>+</sup>, 37); 196 (40). <sup>1</sup>H NMR (CDCl<sub>3</sub>): δ 2.89–3.08 (m, 4H, CH<sub>2</sub>CH<sub>2</sub>), 5.22 (s, 2H, OCH<sub>2</sub>), 6.73–6.77 (d, 1H, *J* = 7.9 Hz, Ar), 6.97–7.26

(m, 8H, Ar), 7.86 (d, 2H, *J* = 6.2 Hz, Py), 8.77 (d, 2H, *J* = 6.2 Hz, Py). <sup>13</sup>C NMR (CDCl<sub>3</sub>): δ 157.77, 154.33, 141.11, 140.36, 130.09, 129.91, 127.85, 127.71, 126.89, 125.40, 123.45, 121.71, 111.17, 66.93, 36.08, 31.37. Anal. (C<sub>20</sub>H<sub>19</sub>NO·HCl) C, H, N. UV-vis (solvent: PBS) λ = 230 nm, ε = 13260.

**4-[[2-(2-(3-Methoxyphenyl)ethyl)phenoxy]methyl]pyridine (17b).** The oil **17b** was transformed to the hydrochloride salt, a white solid (158 mg, 0.44 mmol, 51% yield). Mp: 117–119 °C. MS *m/z* 319 (M<sup>+</sup>, 100); 240 (35). <sup>1</sup>H NMR (CDCl<sub>3</sub>): δ 2.91–3.10 (m, 4H, CH<sub>2</sub>CH<sub>2</sub>), 3.75 (s, 3H, OCH<sub>3</sub>), 5.25 (s, 2H, OCH<sub>2</sub>), 6.67–6.88 (m, 4H, Ar), 7.00–7.29 (m, 4H, Ar), 7.92 (d, 2H, *J* = 5.8 Hz, Py), 8.82 (d, 2H, *J* = 5.8 Hz, Py). <sup>13</sup>C NMR (CDCl<sub>3</sub>): δ 160.28, 158.90, 155.62, 144.04, 141.65, 131.46, 131.27, 130.02, 128.22, 124.68, 123.15, 121.61, 115.29, 112.41, 111.76, 68.18, 55.93, 37.47, 32.55. Anal. (C<sub>21</sub>H<sub>21</sub>NO<sub>2</sub>·HCl) C, H, N. UV-vis (solvent: PBS) λ = 230 nm, ε = 14690.

**General Procedure To Synthesize Final Compounds 22–24.** To a solution of **21** (100 mg, 0.44 mmol) in acetonitrile (3 mL) in a microwave vial were added the appropriate methoxybenzylchloride (23 mg, 0.15 mmol) and KI (2.4 mg, 0.015 mmol). The vial was sealed and heated in a microwave at 110 °C, 150 W, 200 PSI for 10 min. The cooled reaction mixture was diluted with CH<sub>2</sub>Cl<sub>2</sub> (15 mL) and washed successively with H<sub>2</sub>O. Then, the organic layer was dried and evaporated to dryness.

**N-(2-Methoxybenzyl)-2-[2-(3-methoxyphenyl)ethyl]aniline (22).** The crude product was purified by chromatography, eluting with hexane/CHCl<sub>3</sub> (7:3) to give **22** (44.8 mg, 0.129 mmol, 30% yield). MS *m/z* 348 (M<sup>+</sup>, 84%); 227 (100). <sup>1</sup>H NMR (CDCl<sub>3</sub>): δ 2.72–2.96 (m, 4H, CH<sub>2</sub>CH<sub>2</sub>), 3.76 (s, 3H, OMe), 3.84 (s, 3H, OMe), 4.35 (s, 2H, NCH<sub>2</sub>), 6.65–7.29 (m, 12H, Ar). <sup>13</sup>C NMR (CDCl<sub>3</sub>): δ 159.82, 157.57, 146.0, 143.77, 129.49, 129.13, 128.43, 127.43, 125.83, 120.86, 120.71, 117.31, 114.27, 111.55, 111.10, 110.46, 55.46, 55.31, 43.98, 35.35, 33.53. Anal. (C<sub>23</sub>H<sub>25</sub>NO<sub>2</sub>) C, H, N. UV-vis (solvent: PBS) λ = 230 nm, ε = 16333.

**N-(3-Methoxybenzyl)-2-[2-(3-methoxyphenyl)ethyl]aniline (23).** The crude product was purified by chromatography, eluting with hexane/CHCl<sub>3</sub> (1:1) to give **23** (29.8 mg, 0.086 mmol, 20% yield). MS *m/z* 348 (M<sup>+</sup>, 47); 227 (97). <sup>1</sup>H NMR (CDCl<sub>3</sub>): δ 2.73–2.98 (m, 4H, CH<sub>2</sub>CH<sub>2</sub>), 3.75 (s, 3H, OCH<sub>3</sub>), 3.80 (s, 3H, OCH<sub>3</sub>), 4.28 (s, 2H, NCH<sub>2</sub>), 6.60–6.96 (m, 8H, Ar), 7.07–7.30 (m, 4H, Ar). <sup>13</sup>C NMR (CDCl<sub>3</sub>): δ 160.0, 160.50, 145.77, 143.58, 141.34, 129.76, 129.53, 129.05, 127.49, 120.88, 119.86, 117.64, 114.23, 111.30, 112.77, 110.88, 55.36, 55.29, 48.65, 35.48, 33.42. Anal. (C<sub>23</sub>H<sub>25</sub>NO<sub>2</sub>) C, H, N. UV-vis (solvent: PBS) λ = 230 nm, ε = 16333.

**N-(4-Methoxybenzyl)-2-[2-(3-methoxyphenyl)ethyl]aniline (24).** The crude product was purified by chromatography, eluting with hexane/CHCl<sub>3</sub> (4:6) to give an oil **24**, which was transformed to the hydrochloride salt (26.9 mg, 0.07 mmol, 15% yield). MS *m/z* 348 (M<sup>+</sup>, 70%); 227 (100). <sup>1</sup>H NMR (CDCl<sub>3</sub>): δ 2.75–2.96 (m, 4H, CH<sub>2</sub>CH<sub>2</sub>), 3.75 (s, 3H, OMe), 3.79 (s, 3H, OMe), 4.24 (s, 2H, NCH<sub>2</sub>), 6.71–6.87 (m, 6H, Ar), 7.09–7.28 (m, 6H, Ar). Anal. (C<sub>23</sub>H<sub>25</sub>NO<sub>2</sub>·HCl) C, H, N.

**General Procedure To Synthesize Final Compounds 25–27.** To a solution of **21** (200 mg, 0.88 mmol) in ethanol (10 mL) was added the appropriate dimethoxybenzylaldehyde (146 mg, 0.88 mmol), and the resulting solution was stirred and refluxed for 12 h until the disappearance of the aniline **21**. The reaction mixture was then cooled at 0 °C and treated with a solution of NaBH<sub>4</sub> (33.3 mg, 0.88 mmol) in H<sub>2</sub>O (2 mL). The suspension was stirred at room temperature for 3 h, and then it was concentrated to dryness.

**N-[(2,3-Dimethoxybenzyl)-2-[2-(3-methoxyphenyl)ethyl]aniline (25).** The crude product was purified by chromatography, eluting with hexane/AcOEt (8:2) to give **25** as an oil (93.8 mg, 0.25 mmol, 28% yield). MS *m/z* 378 (M<sup>+</sup>, 65%); 227 (100). <sup>1</sup>H NMR (CDCl<sub>3</sub>): δ 2.72–2.97 (m, 4H, CH<sub>2</sub>CH<sub>2</sub>), 3.76 (s, 3H, OMe), 3.87 (s, 6H, OMe), 4.36 (s, 2H, NCH<sub>2</sub>), 6.65–7.25 (m, 11H, Ar). <sup>13</sup>C NMR (CDCl<sub>3</sub>): δ 160.41, 153.50, 147.95, 146.70, 144.31, 133.82, 130.11, 129.60, 128.05, 126.43, 124.83, 121.62, 121.51, 118.04, 114.81, 112.43, 112.26, 111.55, 61.56, 56.58, 55.91, 44.20,

35.99, 34.06. Anal. (C<sub>24</sub>H<sub>27</sub>NO<sub>3</sub>) C, H, N. UV-vis (solvent: PBS)  $\lambda = 226$  nm,  $\epsilon = 4437$ .

**N-[(3,4-Dimethoxy)benzyl]-2-[2-(3-methoxyphenyl)ethyl]aniline (26).** The crude product was purified by chromatography, eluting with hexane/AcOEt (8:2) to give **26** as an oil (64.2 mg, 0.20 mmol, 22% yield). MS *m/z* 378 (M<sup>+</sup>, 54%); 227 (100). <sup>1</sup>H NMR (CDCl<sub>3</sub>):  $\delta$  2.73–2.96 (m, 4H, CH<sub>2</sub>CH<sub>2</sub>), 3.74 (s, 3H, OMe), 3.86 (s, 3H, OMe), 3.88 (s, 3H, OMe), 4.24 (s, 2H, NCH<sub>2</sub>), 6.64–6.91 (m, 8H, Ar), 7.08–7.26 (m, 3H, Ar). <sup>13</sup>C NMR (CDCl<sub>3</sub>):  $\delta$  159.95, 149.63, 148.72, 145.93, 143.60, 132.40, 129.53, 129.14, 127.51, 125.87, 120.90, 119.97, 117.71, 114.36, 112.01, 111.74, 111.52, 111.01, 56.30, 56.18, 55.31, 48.63, 35.57, 33.42. Anal. (C<sub>24</sub>H<sub>27</sub>NO<sub>3</sub>) C, H, N. UV-vis (solvent: PBS)  $\lambda = 226$  nm,  $\epsilon = 47970$ .

**N-[(3,5-Dimethoxy)benzyl]-2-[2-(3-methoxyphenyl)ethyl]aniline (27).** The crude product was purified by chromatography, eluting with hexane/AcOEt (9:1) to give **27** as an oil (81.8 mg, 0.22 mmol, 24% yield). MS *m/z* 378 (M<sup>+</sup>, 54%); 227 (100). <sup>1</sup>H NMR (CDCl<sub>3</sub>):  $\delta$  2.74–2.99 (m, 4H, CH<sub>2</sub>CH<sub>2</sub>), 3.75 (s, 3H, OMe), 3.78 (s, 6H, OMe), 4.25 (s, 2H, NCH<sub>2</sub>), 6.38 (t, 1H, *J* = 2.4 Hz, Ar), 6.54 (d, 2H, *J* = 2.4 Hz, Ar), 6.61–6.84 (m, 4H, Ar), 7.02–7.24 (m, 4H, Ar). <sup>13</sup>C NMR (CDCl<sub>3</sub>):  $\delta$  161.81, 160.43, 146.37, 144.18, 142.82, 130.15, 129.65, 128.12, 127.87, 126.32, 121.48, 119.62, 118.26, 116.43, 114.83, 112.30, 111.48, 106.17, 99.90, 56.09, 55.89, 49.45, 36.06, 34.06. Anal. (C<sub>24</sub>H<sub>27</sub>NO<sub>3</sub>) C, H, N.

**Biological Method. Cell Lines.** The breast cancer cell line of human origin, MCF-7/Adr (resistant to adriamycin or doxorubicin), was routinely cultured in RPMI 1640 supplemented with 10% fetal bovine serum, 2 mM glutamine, 100 U/mL penicillin, and 100  $\mu$ g/mL streptomycin in a humidified incubator at 37 °C with a 5% CO<sub>2</sub> atmosphere. Caco-2 cells were grown in DMEM medium with 10% heat-inactivated fetal bovine serum, 100 U/mL penicillin, 100  $\mu$ g/mL streptomycin, and 2 mM L-glutamine.

**Permeability Experiments. Preparation of the Caco-2 Monolayer.** This procedure has been previously reported by Leopoldo et al.<sup>29</sup> Briefly, Caco-2 cells were harvested with trypsin-EDTA and seeded onto a MultiScreen Caco-2 assay system at a density of 10 000 cells/well. The culture medium was replaced every 48 h for the first 6 days and every 24 h thereafter, and after 21 days in culture, the Caco-2 monolayer was utilized for the permeability experiments. The trans-epithelial electrical resistance (TEER) of the monolayers was measured daily before and after the experiment by using an epithelial voltohmmeter (Millicell-ERS; Millipore, Billerica, MA). Generally, the TEER values obtained are greater than 1000  $\Omega$  for a 21 day culture.

**Drug Transport Experiment.** The apical to basolateral [*P*<sub>app</sub>(A-B)] and basolateral to apical [*P*<sub>app</sub>(B-A)] permeabilities of drugs were measured at 120 min and at various drug concentrations (1–100  $\mu$ M).<sup>30</sup> Drugs were dissolved in Hank's balanced salt solution (HBSS, pH 7.4) and sterile filtered. After 21 days of cell growth, the medium was removed from filter wells and from the receiver plate. The filter wells were filled with 75  $\mu$ L of fresh HBSS buffer, and the receiver plate was filled with 250  $\mu$ L per well of the same buffer. This procedure was repeated twice, and the plates were incubated at 37 °C for 30 min. After the incubation time, the HBSS buffer was removed, and drug solutions were added to the filter well (75  $\mu$ L). HBSS without the drug was added to the receiver plate (250  $\mu$ L). The plates were incubated at 37 °C for 120 min. After the incubation time, samples were removed from the apical (filter well) and basolateral (receiver plate) sides of the monolayer and then were stored in a freezer (–20 °C) pending analysis.

The concentration of compounds was analyzed using UV-vis spectroscopy.

The apparent permeability (*P*<sub>app</sub>), in units of nanometers per second, was calculated using the following equation:

$$P_{\text{app}} = \left( \frac{V_A}{\text{area} \times \text{time}} \right) \left( \frac{[\text{drug}]_{\text{acceptor}}}{[\text{drug}]_{\text{initial}}} \right)$$

where *V*<sub>A</sub> is the volume (in mL) in the acceptor well, area is the surface area of the membrane (0.11 cm<sup>2</sup> of the well), time is

the total transport time in seconds (7200 s), [drug]<sub>acceptor</sub> is the concentration of the drug measured by UV spectroscopy, and [drug]<sub>initial</sub> is the initial drug concentration (1 × 10<sup>–4</sup> M) in the apical or basolateral wells.

**Cell ATP Availability Assay.** This experiment was performed as reported in the technical sheet of the ATPlite firststep Kit for luminescence ATP detection using Victor3, from PerkinElmer Life Sciences.<sup>31</sup> Caco-2 cells were seeded into a 96 well microplate in 100  $\mu$ L of complete medium at a density of 2 × 10<sup>4</sup> cells/well. The plate was incubated O/N in a humidified atmosphere, 5% CO<sub>2</sub> at 37 °C. The medium was removed, and 100  $\mu$ L of complete medium in the presence or absence of different concentrations of test compounds was added. The plate was incubated for 2 h in a humidified atmosphere, 5% CO<sub>2</sub> at 37 °C. Then, 50  $\mu$ L of mammalian cell lysis solution was added to all wells, and the plate was stirred for 5 min in an orbital shaker. In all wells, 50  $\mu$ L of substrate solution was added, and the plate was stirred for 5 min as above-reported. The plate was dark adapted for 10 min, and the luminescence was measured in Victor3.

**[<sup>3</sup>H]-Vinblastine Transport Inhibition.** Caco-2 cells were seeded onto multiscreen plates, 10 000 cells/well for 21 days, measuring the integrity of the cell monolayers by trans-epithelial electrical resistance (TEER,  $\Omega \times \text{cm}^2$ ) with an epithelial voltohmmeter. A mature Caco-2 cell monolayer exhibited a TEER > 800  $\Omega \times \text{cm}^2$  prior to use in transport experiments. Transport experiments for tested compounds were carried out as described by Taub et al.<sup>32</sup>

In each well to basolateral (BL) compartment, in the absence and in the presence of P-gp inhibitors (from 0.20 to 400  $\mu$ M) was added 20 nM [<sup>3</sup>H]-vinblastine for 120 min at 37 °C, and its appearance in the apical (AP) compartment was monitored. At 120 min, a 20  $\mu$ L sample was taken from the donor compartment to determine the concentration of radioligand remaining in the donor chamber at the end of the experiment. Samples were analyzed by using a LS6500 Beckman counter. For each compound, [<sup>3</sup>H]-vinblastine transport inhibition was calculated as the radioactivity difference between radioligand in the presence and absence of compound. These differences were expressed as a percentage of inhibition effect for each single drug concentration.

**[<sup>3</sup>H]-Mitoxantrone Transport Inhibition.** Caco-2 cells were seeded onto multiscreen plates, 10 000 cells/well for 21 days, measuring the integrity of the cell monolayers by trans-epithelial electrical resistance (TEER,  $\Omega \times \text{cm}^2$ ) with an epithelial voltohmmeter. A mature Caco-2 cell monolayer exhibited a TEER > 800  $\Omega \times \text{cm}^2$  prior to use in transport experiments. Transport experiments for tested compounds were carried out as described by Taub et al.<sup>32</sup>

In each well to basolateral (BL) compartment, in the absence and in the presence of P-gp inhibitors (from 0.20 to 400  $\mu$ M) was added 20 nM [<sup>3</sup>H]-mitoxantrone for 120 min at 37 °C, and its appearance in the apical (AP) compartment was monitored. At 120 min, a 20  $\mu$ L sample was taken from the donor compartment to determine the concentration of radioligand remaining in the donor chamber at the end of the experiment. Samples were analyzed by using a LS6500 Beckman counter. For each compound, [<sup>3</sup>H]-mitoxantrone transport inhibition was calculated as the radioactivity difference between radioligand in the presence and absence of compound. These differences were expressed as a percentage of inhibition effect for each single drug concentration.

**Cytotoxicity Assay.** The assay was performed by using the CytoTox-One kit from the Promega Corp. (Madison, WI), as reported in a previous paper.<sup>33</sup> Cell death was determined as the release of lactate dehydrogenase (LDH) into the culture medium. The percentage of cytotoxicity was calculated relative to the LDH release from total lysis of cells in the untreated control. It is assumed here that the drug-treated wells and the control wells contained the same total number of cells (dead plus alive cells) at the end of the treatment period. Therefore, the cytotoxic effect of tested compounds was unaffected by any underestimation of cytotoxicity that could occur because of the decreased total number of cells in the treated samples as compared to that of the untreated control. Cells

were seeded into 96 well plates for optical performance in the fluorescent cell-based assay in 100  $\mu$ L of complete medium in the presence or absence of different concentrations of test compounds. The plate was incubated for 24 h in a humidified atmosphere, 5% CO<sub>2</sub> at 37 °C, and then 100  $\mu$ L of substrate mix in assay buffer was added. Lysis solution (10  $\mu$ L) was added to the untreated wells in order to estimate total LDH. Plates were kept protected from light for 10 min at room temperature, and 50  $\mu$ L of stop solution was added to all wells. The fluorescence was recorded using a PerkinElmer LS55 luminescence spectrometer with a 560 nm excitation wavelength and a 590 nm emission wavelength. The cytotoxicity percentage was estimated as follows:

$$100(\text{LDH in medium of treated cells} - \text{culture medium background}) / (\text{total LDH in untreated cells} - \text{culture medium background})$$

**Statistical Analysis.** The EC<sub>50</sub> values of the compounds reported in Tables 1 and 2 were determined by nonlinear curve fitting utilizing the GraphPad Prism program.<sup>34</sup>

**Supporting Information Available:** Elemental analysis of compounds **11a,b**, **13a,b**, **14a,b**, **15a,b**, **16a,b**, **17a,b**, and **22–27** and experimental section for key intermediates **18**, **20**, and **21**. This material is available free of charge via the Internet at <http://pubs.acs.org>.

## References

- (1) Klein, I.; Sarkadi, B.; Varadi, A. An inventory of the human ABC proteins. *Biochim. Biophys. Acta* **1999**, *1461*, 237–262.
- (2) Ambudkar, S. V.; Dey, S.; Hrycyna, C. A.; Ramachandra, M.; Pastan, I.; Gottesman, M. M. Biochemical, cellular, and pharmacological aspects of the multidrug transporter. *Annu. Rev. Pharmacol. Toxicol.* **1999**, *39*, 361–398.
- (3) Ayrton, A.; Morgan, P. Role of transport proteins in drug absorption, distribution, and excretion. *Xenobiotica* **2001**, *31*, 469–497.
- (4) Dean, M.; Rzhetsky, A.; Allikmets, R. The human ATP-binding cassette (ABC) transporter superfamily. *Genome Res.* **2001**, *11*, 1156–1166.
- (5) Hyde, S. C.; Emsley, P.; Hartshorn, M. J.; Mimmack, M. M.; Gileadi, U.; Pearce, S. R.; Gallagher, M. P.; Gill, D. R.; Hubbard, R. E.; Higgins, C. F. Structural model of ATP-binding proteins associated with cystic fibrosis, multidrug resistance, and bacterial transport. *Nature* **1990**, *346*, 362–365.
- (6) Quinton, P. M. Physiological basis of cystic fibrosis: a historical perspective. *Physiol. Rev.* **1999**, *79*, S3–S22.
- (7) Remaley, A. T.; Rust, S.; Rosier, M.; Knapper, C.; Naudin, L.; Broccardo, C.; Peterson, K. M.; Koch, C.; Arnould, I.; Prades, C.; Duverger, N.; Funke, H.; Assman, G.; Dinger, M.; Dean, M.; Chimini, G.; Santamarina-Fojo, S.; Fredrickson, D. S.; Deneffe, P.; Bryan, H.; Brewer, H. B. Human ATP-binding cassette transporter 1 (ABC1): genomic organization and identification of the genetic defect in the original Tangier disease kindred. *Proc. Natl. Acad. Sci. U.S.A.* **1999**, *96*, 12685–12690.
- (8) Brooks-Wilson, A.; Marcil, M.; Clee, S. M.; Zhang, L. H.; Roomp, K.; van Dam, M.; Yu, L.; Brewer, C.; Collins, J. A.; Molhuizen, H. O.; Louber, O.; Ouellette, B. F.; Fichter, K.; Ashbourne-Excoffon, K. J.; Sensen, C. W.; Scherer, S.; Mott, S.; Denis, M.; Martindale, D.; Frohlich, J.; Morgan, K.; Koop, B.; Pimstone, S.; Kastelein, J. J.; Genest, J.; Hayden, M. R. Mutations in ABC1 in Tangier disease and familial high-density lipoprotein deficiency. *Nat. Genet.* **1999**, *22*, 336–345.
- (9) Bates, E. S.; Robey, R.; Knutsen, T.; Honjo, Y.; Litman, T.; Dean, M. New ABC transporters in multi-drug resistance. *Emerging Ther. Targets* **2000**, *4*, 561–580.
- (10) Gottesman, M. M.; Fojo, T.; Bates, S. E. Multidrug resistance in cancer: role of ATP-dependent transporters. *Nat. Rev. Cancer* **2002**, *2*, 48–58.
- (11) Schneider, E.; Paul, D.; Ivy, P.; Cowan, K. H. Multidrug resistance. *Cancer Chemother. Biol. Response Modif.* **1999**, *18*, 152–177.
- (12) Glavinas, H.; Krajcsi, P.; Cserepes, J.; Sarkadi, B. The role of ABC transporters in drug resistance, metabolism, and toxicity. *Curr. Drug Delivery* **2004**, *1*, 27–42.
- (13) Krishna, R.; Mayer, L. D. Multidrug resistance (MDR) in cancer. Mechanisms, reversal using modulators of MDR, and the role of MDR modulators in influencing the pharmacokinetics of anticancer drugs. *Eur. J. Pharm. Sci.* **2000**, *11*, 265–283.
- (14) Leslie, E. M.; Deeley, R. G.; Cole, S. P. C. Multidrug resistance proteins: role of P-glycoprotein MRP1, MRP2, and BCRP (ABCG2) in tissue defense. *Toxicol. Appl. Pharmacol.* **2005**, *204*, 216–237.
- (15) Nobili, S.; Landini, I.; Gigliani, B.; Mini, E. Pharmacological strategies for overcoming multidrug resistance. *Curr. Drug Targets* **2006**, *7*, 861–879.
- (16) Thomas, H.; Coley, H. M. Overcoming multidrug resistance in cancer: an update on the clinical strategy of inhibiting P-glycoprotein. *Cancer Control* **2003**, *10*, 159–165.
- (17) Pérez-Tomás, R. Multidrug resistance: retrospect and prospects in anticancer drug treatment. *Curr. Med. Chem.* **2006**, *13*, 1859–1876.
- (18) Teodori, E.; Dei, S.; Martelli, S.; Scapecchi, F.; Gualtieri, F. The functions and structure of ABC transporters: implications for the design of new inhibitors of P-gp and MRP1 to control multidrug resistance (MDR). *Curr. Drug Targets* **2006**, *7*, 893–909.
- (19) Avendano, C.; Menendez, J. C. Inhibitors of multidrug resistance to antitumor agents (MDR). *Curr. Med. Chem.* **2002**, *9*, 159–193.
- (20) Planting, A. S.; Sonneveld, P.; van der Gaast, A.; Sparreboom, A.; van der Burg, M. E.; Luyten, G. P.; de Leeuw, K.; de Boer-Dennert, M.; Wissel, P. S.; Jewell, R. C.; Paul, E. M.; Purvis, N. B.; Verweij, J. A phase I and pharmacologic study of the MDR converter GF120918 in combination with doxorubicin in patients with advanced solid tumors. *Cancer Chemother. Pharmacol.* **2005**, *55*, 91–99.
- (21) Morschhauser, F.; Zinzani, P. L.; Burgess, M.; Sloots, L.; Bouafia, F.; Dumontet, C. Phase I/II trial of a P-glycoprotein inhibitor, Zosuquidar.3HCl trihydrochloride (LY335979), given orally in combination with the CHOP regimen in patients with non-Hodgkin's lymphoma. *Leuk. Lymphoma* **2007**, *48*, 708–715.
- (22) Modok, S.; Mellor, H. R.; Callaghan, R. Modulation of multidrug resistance efflux pump activity to overcome chemoresistance in cancer. *Curr. Opin. Pharmacol.* **2006**, *6*, 350–354.
- (23) Colabufo, N. A.; Berardi, F.; Perrone, R.; Rapposelli, S.; Digiacomio, M.; Balsamo, A. Arylmethyloxyphenyl derivatives: small molecules displaying P-glycoprotein inhibition. *J. Med. Chem.* **2006**, *49*, 6607–6613.
- (24) Polli, J. W.; Wring, S. A.; Humphreys, J. E.; Huang, L.; Morgan, J. B.; Webster, L. O.; Serabjit-Singh, C. S. Rational use of in vitro P-glycoprotein assays in drug discovery. *J. Pharmacol. Exp. Ther.* **2001**, *299*, 620–628.
- (25) Romera, J. L.; Cid, J. M.; Trabanco, A. A. Potassium iodide catalysed monoalkylation of anilines under microwave irradiation. *Tetrahedron Lett.* **2004**, *45*, 8797–8800.
- (26) Seelig, A.; Gatlik-Landwojtowicz, E. Inhibitors of multidrug efflux transporters: their membrane and protein interactions. *Mini-Rev. Med. Chem.* **2005**, *5*, 135–151.
- (27) Pleban, K.; Ecker, G. F. Inhibitors of P-glycoprotein-lead identification and optimisation. *Mini-Rev. Med. Chem.* **2005**, *5*, 153–163.
- (28) Balimane, P. V.; Chong, S. A combined cell based approach to identify P-glycoprotein substrates and inhibitors in a single assay. *Int. J. Pharm.* **2005**, *301*, 80–88.
- (29) Leopoldo, M.; Lacivita, E.; De Giorgio, P.; Colabufo, N. A.; Niso, M.; Berardi, F.; Perrone, R. Design, synthesis, and binding affinities of potential positron emission tomography (PET) ligands for visualization of brain dopamine D3 receptors. *J. Med. Chem.* **2006**, *49*, 358–365.
- (30) Rautio, J.; Humphreys, J. E.; Webster, L. O.; Balakrishnan, A.; Keogh, J. P.; Kunta, J. R.; Serabjit-Singh, J.; Polli, J. W. In vitro P-glycoprotein inhibition assays for assessment of clinical drug interaction potential of new drug candidates: a recommendation for probe substrates. *Drug Metab. Dispos.* **2006**, *34*, 786–792.
- (31) Kangas, L.; Grönroos, M.; Nieminen, A. L. Bioluminescence of cellular ATP: a new method for evaluating agents in vitro. *Med. Biol.* **1984**, *62*, 338–343.
- (32) Taub, M. E.; Podila, L.; Almeida, I. Functional assessment of multiple P-glycoprotein (P-gp) probe substrate: influence of cell line and modulator concentration on P-gp activity. *Drug Metab. Dispos.* **2005**, *33*, 1679–1687.
- (33) Colabufo, N. A.; Berardi, F.; Contino, M.; Niso, M.; Abate, C.; Perrone, R.; Tortorella, V. Antiproliferative and cytotoxic effects of some  $\sigma_1$  antagonists in tumour cell lines. *Naunyn-Schmiedeberg's Arch. Pharmacol.* **2004**, *370*, 106–113.
- (34) GraphPad Prism Software, version for Windows; GraphPad Software, Inc.: San Diego, CA, 1998.

JM701267Q